Computer Analysis of a Polymer Coating Exposed to Field Weather Conditions

Doug Burch, Jonathan W. Martin, and Mark R. VanLandingham—National Institute of Standards and Technology*

INTRODUCTION

O
utdoor exposure of polymeric materials causes almost all materials to degrade. Degradation in the presence of solar ultraviolet radiation can occur in several ways. First, photons from the ultraviolet (UV) portion of the solar spectrum are absorbed by an exposed material causing photolytic degradation to occur. Photolytic degradation has been shown in the laboratory to be enhanced under elevated relative humidity and temperature conditions.[1] Second, surface wetting by rain and dew condensation, which can saturate an exposed polymeric material, can be followed by rapid drying due to incident solar radiation. This process causes rapid fluctuations in moisture content and relative humidity[†] of the material. Humidity fluctuations can cause a polymeric material to expand and contract resulting in internal stress fluctuations and fatigue-stress degradation. Third, the presence of liquid water accelerates chemical reactions (e.g., hydrolysis), particularly under conditions of elevated temperature. Finally, variations in outdoor temperature and incident solar radiation can cause an exposed polymeric material to undergo diurnal temperature cycles resulting in thermal expansion and contraction. As with humidity, temperature fluctuations can potentially cause fatigue-stress degradation, and high temperatures can accelerate the chemical degradation processes.

Burch and Martin[2] previously showed that the moisture and heat transfer model used at the National Institute of Standards and Technology (NIST), called MOIST 3.0,[3] could be successfully applied to predict the temperature and moisture content of a polymer coating exposed outdoors. However, MOIST 3.0 did not include the important effects of exterior surface wetting by rain and dew condensation. Moreover, it used a constant convection coefficient at the exposed surface. The model also did not account for effects due to the local wind speed. A new model, called MOIST 4.0, was developed to overcome these limitations.

In this paper, a new heat and moisture transfer model (MOIST 4.0) is presented that predicts the temperature, moisture content, and relative humidity through the thick-

A heat and moisture transfer model was used to study weathering of polymeric materials, such as paint, asphalt, sealants, plastics, textiles, and polymeric composites. Three damage indices, related to temperature changes, humidity changes, and time of wetness, respectively, were introduced to quantify adverse effects of climate. The variation of these indices was investigated for a hot and humid climate (Miami, FL) and a hot and dry climate (Phoenix, AZ). In addition, the relative effects of solar radiation, surface wetting by rain and dew condensation, and variations in outdoor temperature and relative humidity on the three damage indices were investigated.

ness of an exposed paint layer. First, the model theory is presented, followed by enhancements to MOIST 3.0. Input parameters and damage indices are then described. Finally, the results of two simulations corresponding to hot-wet and hot-dry environments are discussed, followed by the summary and conclusions.

MODEL THEORY

Assumptions

Some of the more important assumptions of the analysis are:

- heat transfer and moisture transfer are one-dimensional
- snow accumulation on horizontal surfaces and its effect on the solar absorptance and thermal resistance are neglected
- heat transport by liquid movement is neglected.

D. Burch, J.W. Martin, and M.R. VanLandingham

Physical Laws

The water vapor transfer rate, η_v, can be predicted by Fick's law with vapor pressure, p, serving as a transport potential, or:

$$\eta_v = -\mu \frac{\partial p}{\partial y} \tag{1}$$

Here y is the coordinate direction perpendicular to the surface and μ is the vapor permeability. The liquid transfer rate, η_l, can also be predicted by Fick's law with moisture content, γ, serving as a transport potential, or:

$$\eta_l = -\rho_d D \frac{\partial y}{\partial y} \tag{2}$$

where D is the liquid diffusivity and ρ_d is the dry material density. The relative saturation, s, is then defined by the relation:

$$s = \frac{\gamma - \gamma_{97}}{\gamma_s - \gamma_{97}} \quad (\gamma > \gamma_{97}) \tag{3}$$

where γ_s is the capillary saturated moisture content and γ_{97} is the equilibrium moisture content at a relative humidity of 97%. Above a relative humidity of 97%, the large pores of the material are being filled with water (as predicted by the Kelvin equation), and capillary transport occurs. For a relative humidity below 97%, capillary transport does not occur and the calculation is not performed. The relative saturation takes on a value of 0 at the onset of capillary transfer and has a value of 1 after the material becomes saturated with water. Performing a change of variable, equation (2) can be rewritten as:

$$\eta_l = -\rho_d D' \frac{\partial s}{\partial y} \tag{4}$$

where the modified liquid diffusivity, D', is defined by:

$$D' = D(\gamma_s - \gamma_{97}) \tag{5}$$

The heat transfer rate, q, can be predicted by Fourier's law, or:

$$q = -k \frac{\partial T}{\partial y} \tag{6}$$

where T is temperature and k is the thermal conductivity. These physical laws, as given in equations (1), (2), and (6), are consistent with those of the International Energy Agency Annex 24.[4]

Transport Equations

Within a polymer material or a layer of a building envelope, the moisture distribution is governed by the following conservation of mass equation:

$$\frac{\partial}{\partial y}\left(\mu \frac{\partial p}{\partial y}\right) + \frac{\partial}{\partial y}\left(\rho_d D' \frac{\partial s}{\partial y}\right) = \rho_d \frac{\partial \gamma}{\partial t} \tag{7}$$

The first term on the left side of equation (7) represents water vapor diffusion, whereas the second term represents capillary (liquid) transfer. The right side of equation (7) represents moisture storage within the material where t is time. The sorption isotherm (i.e., the relationship between equilibrium moisture content and relative humidity) is used as the constitutive relation in solving equation (7). When the temperature is below freezing, capillary

transfer does not occur, and the modified liquid diffusivity is zero. Freezing point depression in the small pores is neglected. Also, for many polymer systems, moisture absorption occurs via water vapor diffusion only such that the second term in equation (7) would be negligible. However, equation (7) can also be used to account for liquid transfer that occurs in multicomponent polymer systems (e.g., water diffusion into microcracks). Thus, this model can account for moisture diffusion under a wide variety of exposure and material conditions.

The temperature distribution is calculated from the following conservation of energy equation:

$$\frac{\partial}{\partial y}\left(k \frac{\partial T}{\partial y}\right) + h_{lv} \frac{\partial}{\partial y}\left(\mu \frac{\partial p}{\partial y}\right) = \rho_d(c_d + \gamma c_w)\frac{\partial T}{\partial t} \tag{8}$$

The first term on the left side of equation (8) represents conduction, whereas the second term is the latent heat transfer derived from phase change associated with the movement of moisture. The right side of equation (8) represents the storage of heat within the material and accumulated moisture. Other symbols in the above equation include the dry specific heat of the material (c_d), the specific heat of water (c_w), and the latent heat of vaporization (h_{lv}).

In equation (7), the water vapor permeability, μ, and the modified liquid diffusivity, D', are strong functions of moisture content. In equation (8), the thermal conductivity, k, is a function of temperature and moisture content.

Boundary Conditions

When the upper exposed surface is not wet, the mass transfer rate across a convective boundary layer is set equal to the rate of water vapor diffusion into the surface, or:

$$h_m(p_o - p_s) = -\mu \frac{\partial p}{\partial y} \tag{9}$$

The derivative of the vapor pressure is evaluated at the surface. The symbols p_o and p_s refer to the water vapor pressure of the outdoor air and the exposed surface, respectively. The symbol h_m is the vapor mass transfer coefficient. When the surface is wet due to either dew condensation or rain, the relative saturation (s) at the surface is one, and the water vapor pressure at the surface is saturated.

Treating the exposed surface as a control volume, the conservation of energy principle can be applied. The absorbed solar radiation less the heat conducted into the surface is set equal to the heat loss to the outdoor air by convection and radiation, or:

$$-k\frac{\partial T}{\partial y} + \alpha H_{sol} = h_{c,o}(T_s - T_o) + h_{r,o}(T_s - T_{sky}) \tag{10}$$

where T_s = the surface temperature, T_o = outdoor ambient temperature, T_{sky} = equivalent black body temperature of the sky. The derivative of temperature is evaluated at the surface. Here $h_{r,o}$ is the radiation heat transfer coefficient defined by the relation:

$$h_{r,o} = E\sigma(T_s + T_{sky})(T_s^2 + T_{sky}^2) \tag{11}$$

where E = emittance factor which includes the surface emissivity and the view factor from the outdoor surface to the sky. The solar radiation, H_{sol}, incident onto exterior

surfaces having arbitrary tilt and orientation was predicted using algorithms given in Duffie and Beckman[5] and α is the solar absorptance at the exterior surface. All temperatures in the above equation are absolute temperatures.

Applications

By changing the boundary conditions at the surface opposite the exposed surface, the new model has the capability to simulate both an outdoor exposure site application and a building envelope application. For the outdoor exposure site application, the ambient temperature and vapor pressure of the underside of a test panel are assumed to be the same as those for the upper exposed surface. However, the surface is shaded from sunlight and receives no direct solar radiation. The vapor mass transfer rate through a convective boundary layer is equated to the diffusion transfer rate into the panel surface, or

$$h_m(p_o - p_s) = -\mu \frac{\partial p}{\partial y} \qquad (12)$$

where p_s is the water vapor pressure at the surface, p_o is the outdoor vapor pressure, and the derivative of the vapor pressure is evaluated at the surface. Similarly, the convective heat transfer rate is equated to the rate of heat conducted into the surface, or:

$$h_c(T_o - T_s) = -k \frac{\partial T}{\partial y} \qquad (13)$$

where h_c = convective heat transfer coefficient at the surface. The derivative of the temperature is evaluated at the surface.

For a building envelope application, the surface opposite the exposed surface is the interior surface of a building. The indoor temperature and relative humidity are those of the indoor air. At this surface, the vapor transfer rate through an air film and paint layer (or wallpaper) is equated to the diffusion transfer rate into the material surface, or:

$$M_{e,i}(p_i - p_s) = -\mu \frac{\partial p}{\partial y} \qquad (14)$$

where the derivative of the vapor pressure is evaluated at the surface. Here p_i is the water vapor pressure of the indoor air and $M_{e,i}$ is an effective vapor conductance that accounts for the effect of a thin paint (or wallpaper) layer. This effective vapor conductance is composed of a surface conductance, $M_{p,i}$, associated with the paint (or wallpaper) layer in series with the convective mass transfer coefficient, $h_{m,i}$, associated with the air film and is given by:

$$M_{e,i} = \frac{1}{\dfrac{1}{h_{m,i}} + \dfrac{1}{M_{p,i}}} \qquad (15)$$

At the same boundary, the heat transfer rate through the air film is equated to the heat conduction rate into the surface, or:

$$(h_{r,i} + h_{c,i})(T_i + T_s) = -k \frac{\partial T}{\partial y} \qquad (16)$$

where the derivative of the temperature is evaluated at the surface. Here $h_{r,i}$ and $h_{c,i}$ are the radiation and convective conductance of the inside surface boundary layer, T_i is the

indoor air temperature, and the thermal resistance of the paint layer has been ignored.

The user of the model can conduct simulations using a constant or variable indoor relative humidity. For the constant indoor relative humidity, the user specifies an indoor temperature and relative humidity that are held constant during the entire simulation. For the variable indoor relative humidity, the user specifies a house effective leakage area (ELA) and an indoor moisture generation rate. The indoor relative humidity during the winter is permitted to vary and is calculated from a moisture balance of the whole building. The winter and summer indoor temperatures are set to separate constant values. The variable indoor relative humidity model provides more realistic simulations that are believed to more closely coincide with actual field conditions. The variable indoor relative humidity model is described in detail by Burch and Chi.[3]

Adjacent Layers

The temperature, water vapor pressure, and relative moisture content are continuous at the boundary between adjacent material layers. When liquid transfer occurs across the boundary between two different materials, the natural logarithm of the capillary pressure is generally considered to be continuous.[6] Richards[7] measured the capillary pressure for four different materials, the natural logarithms of which are plotted versus relative saturation in *Figure* 1. The shape of the curve at low relative saturation is required to comply with theoretical considerations. Note that the four materials are correlated by the same relationship, thereby indicating a one-to-one correspondence between the natural logarithm of capillary pressure and relative saturation. Therefore, if the natural logarithm of capillary pressure is continuous, then the relative saturation should also be continuous at the boundary between different materials.
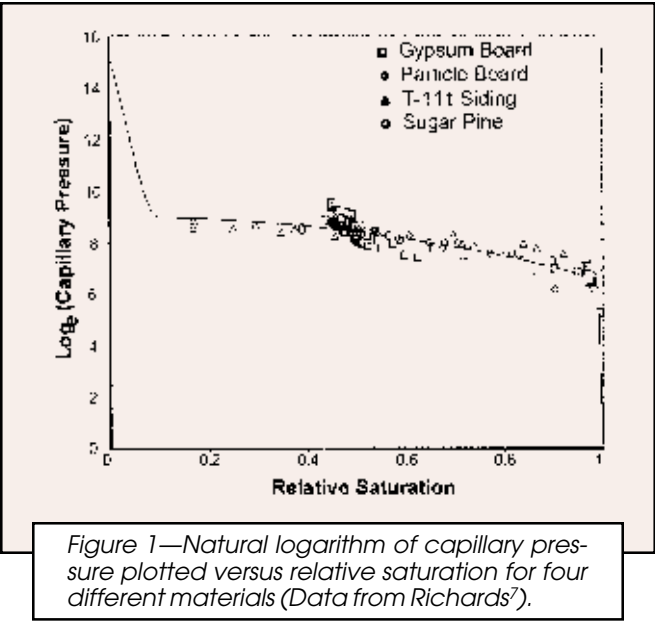
Solution Procedure

Implicit finite difference equations were developed to represent the basic moisture and heat transport equations [equations (7) and (8), respectively]. The finite difference equations were solved using an efficient tridiagonal matrix solution technique. The user can specify up to 500 finite difference nodes. For most polymer material applications, a 0.01 hr time step is required to achieve stability of the mathematical solution. However, the user has the option to vary the time step.

MODEL ENHANCEMENTS

In developing the above new model, the computer code for MOIST 3.0 was used as a starting point and the following enhancements were incorporated into the model to create MOIST 4.0.

Surface Wetting by Rain and Dew Condensation

The upper exposed surface is assumed to be wet when either rain occurs or the surface temperature falls below the outdoor dew point temperature. When either of these conditions occurs, the relative saturation at the surface is equal to 1.0 and capillary transport into the surface is

D. Burch, J.W. Martin, and M.R. VanLandingham

Figure 1—Natural logarithm of capillary pressure plotted versus relative saturation for four different materials (Data from Richards[7]).

allowed. Additionally, the water vapor pressure at the surface is saturated, and elevated water vapor transport into the surface occurs. Excess water, not transported into the surface, is assumed to run off the surface. New capillary algorithms were developed to accommodate capillary transport associated with surface wetting.

In the previous MOIST computer program (Release 3.0), capillary (liquid) transfer was modeled using capillary pressure as a potential with the hydraulic conductivity serving as a transport coefficient. When these capillary algorithms were modified to accommodate surface wetting, achieving convergence of the mathematical solution became difficult, and the model frequently became unstable. This instability was caused by the variation of the transport coefficients over an enormous range when the

surface material changed very rapidly from a dry state to a fully wet state at the wetted surface. A very large number of nodes with an extremely small time step were required to achieve convergence, thereby requiring excessive amounts of computer time. To overcome this difficulty, the liquid transport term in the conservation of mass equation [equation (7)] was modified. The relative saturation was used as the potential for transferring liquid water with the modified diffusivity serving as a transport coefficient. In this formulation, the capillary transport coefficients were considerably less variable, thereby resulting in a considerably more stable mathematical solution.

Variable Convection as a Function of Wind Speed

The rate of convection at the exposed polymer surface was corrected for the ground boundary layer. The wind speed at meteorological stations is measured at a height of 10 m (33 ft) above the ground. The local wind speed, U, at a test panel of an outdoor exposure site, typically located at a height $H = 0.92$ m (3.0 ft) above the ground, was predicted by the relation[8]:

$$U = U_{ref}(H/H_{ref})^a \qquad (17)$$

where U_{ref} is the reference wind speed of a meteorological station measured at the reference height, H_{ref}. The exponent a is an empirical constant equal to 0.14.[8] When the measured parameters for an outdoor weathering site are used instead of either WYEC*,[9] or TMY2[10] data, then H_{ref} is the height at which the weather data is measured. The local heat transfer coefficient and mass transfer coefficient were calculated from the local wind speed using relations found in ASHRAE.[8]

---

*The computer model is able to input the old WYEC weather data. ASHRAE has released new weather data called WYEC2, but the computer model does not currently have the capability to read this new weather data.

Table 1—Material Properties for Alkyd Resin Paint

Property Description	Coefficient			Units
Sorption Isotherm	A_1	=	0.0174	kg_w/kg_d
	A_2	=	4.71	—
$\gamma = \dfrac{A_1 rh}{(1+A_2 rh)(1-A_3 rh)}$	A_3	=	0.943	—
Liquid Diffusivity	B_1	=	1.62×10^{-12}	m^2/s
	B_2	=	0.0	—
$D = B_1 Exp(B_2 \cdot \gamma)$				
Capillary Saturated Moisture Content	γ_s	=	0.106	kg_w/kg_d
Thermal Conductivity	k_d	=	0.78	$W/m°C$
$k = k_d + C_T(T-T_R) + C_\gamma \gamma$	C_T	=	0.0	$W/m°C$ per°C
	C_γ	=	0.0	$W/m°C$ per kg_w/kg_d
Dry Density	ρ_d	=	1,640	kg/m^3
Specific Heat	c	=	1,256	$J/kg·K$
Vapor Permeability	C_1	=	1.62×10^{-13}	m^2/s
$\mu = C_1 + C_2 \cdot Exp(C_3 \cdot rh)$	C_2	=	0.0	m^2/s
	C_3	=	0.0	—

Note: In this table, the heat and moisture and heat transport coefficients are constant. In real materials, the moisture and heat transfer coefficients are dependent upon moisture content and temperature. The authors were unable to include these dependencies in the analysis because appropriate parameter values pertaining to these dependencies for an alkyd-resin paint were unavailable in the literature.

Improved Sky Temperature Algorithm

The clear sky temperature was modeled using an equation developed by Bliss.[11] The sky temperature for a partly cloudy sky was estimated using the approximate relation:

$$T_{sky} = T_{sky,clear}(1 - TCC) + T_o \cdot TCC \qquad (18)$$

where $T_{sky,clear}$ is the clear sky temperature and TCC is the total cloud cover expressed as a fraction. Total cloud cover is available in both the Weather Year for Energy Calculations (WYEC) and Typical Meteorological Year (TMY) weather data. When $TCC = 1$ (completely cloudy sky), the sky temperature is equal to the outdoor air temperature. When TCC = 0 (a clear sky), the sky temperature is equal to the clear sky temperature.

Simulation of Variable Permeance Paint Layers

For building envelope applications, algorithms were incorporated into the computer program to permit the permeance of the paint to be variable dependent upon the average relative humidity (rh) across the layer. The paint permeance (M) was modeled using the following relationship[12]:

$$M = A_1 + A_2 \, exp(A_3 \cdot rh) \qquad (19)$$

where A_1, A_2, and A_3 are empirical constants determined from a series of measurements.

Capability of Using Measured Parameters For an Outdoor Exposure Site

The new computer program can utilize parameters measured at an outdoor exposure site in place of WYEC or TMY weather data. The outdoor weather parameters that can be input into the program include the following (the necessary unit of each particular parameter is in parenthesis where applicable): month, day, hour, ambient temperature (°C), relative humidity (%), wind speed (km/h), wind direction (degrees from North), incident total hemispherical solar radiation onto the test plane (MJ/m²), and time of wetness (wet surface = 1.0).

INPUT PARAMETERS

Description of Base Case

In the computer simulations that follow, analysis was performed for a 0.27 mm thick alkyd resin paint* applied to a 3.2 mm thick plastic panel sloped at 5° from the horizontal and facing South. The thermal emittance and solar absorptance of the exposed paint surface were 0.9 and 0.7, respectively. Many common paints have a thermal emittance near 0.9.[13] Solar absorptance depends on color, and a value of 0.7 corresponds to a medium-colored surface. The solar absorptance of building materials generally range from about 0.3 (light colored surface) to about 0.9 (dark colored surface) [see Table 389, reference 13].

Polymer Coating Material Properties

The material properties of the alkyd resin paint are listed in *Table* 1. The sorption isotherm, capillary satu-

*The thickness was based on the mean free films studied by Rosen and Martin.[14] However, a more typical thickness would have been 0.13 to 0.15 mm.)
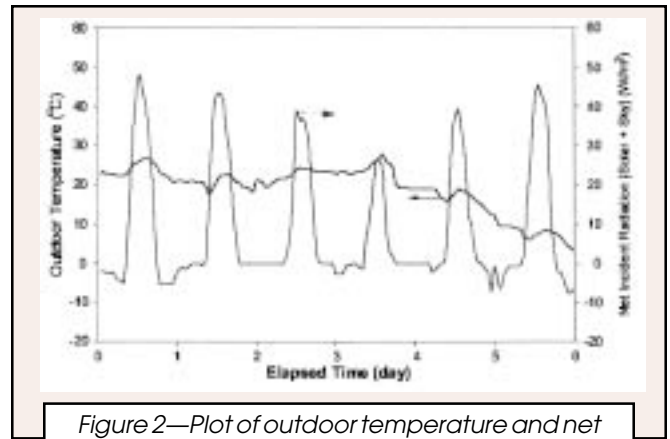

Figure 2—Plot of outdoor temperature and net incident radiation (solar + sky) versus elapsed time for the illustrative six-day winter period in Miami, FL.

rated moisture content, and vapor permeability were based on Rosen and Martin.[14] The effect of hysteresis in the sorption isotherm was neglected and a mean value between the adsorption and desorption isotherm was used in the analysis consistent with other models reported in IEA Annex 24.[4] The other properties were based on information found in reference 15.

Definition of Damage Indices

In the simulation results to be discussed, damage indices were used to quantify several adverse effects of the outdoor climate. A higher damage index corresponds to a more adverse outdoor climate and a larger potential for degradation. The term "damage index" is intentionally used instead of "damage function," which implies the existence of a precise quantitative relationship between the parameter and the amount of degradation, which is not the case for the indices used in this model.

Mean Diurnal Temperature Change Index

The mean diurnal temperature change index (I_T) is defined as the mean amplitude of the diurnal temperature
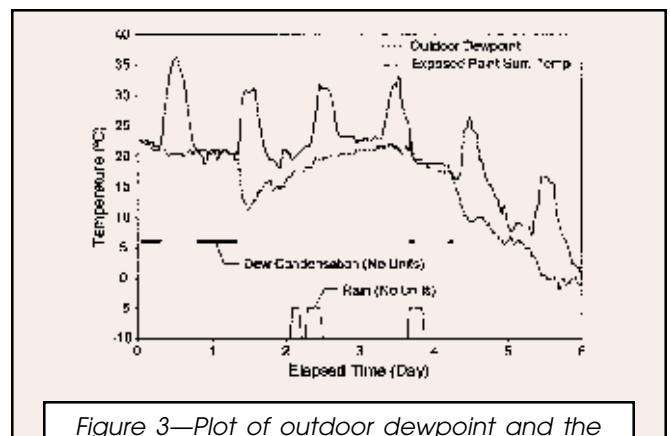

Figure 3—Plot of outdoor dewpoint and the calculated surface temperature of the exposed paint, in which the determination of the time periods of dew condensation is shown for the illustrative six-day winter period in Miami, FL. Also shown are the time periods when rain occurred.
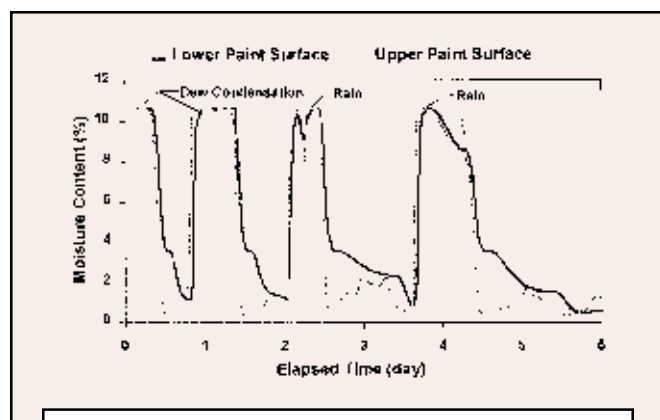
Figure 4—Plot of moisture content at the polymer coating surfaces versus elapsed time for the illustrative six-day winter period in Miami, FL.

Figure 5—Plot of relative humidity at the polymer coating surfaces versus elapsed time for the illustrative six-day winter period in Miami, FL.

cycles at the exposed paint surface during a given time period. The amplitudes (difference between the maximum and minimum diurnal surface temperatures) for the surface temperature cycles are determined, and the arithmetic mean for these amplitudes is subsequently calculated. Diurnal temperature swings of the exposed paint surface are believed to produce expansion/contraction cycles that can lead to fatigue-stress degradation of a paint layer.

Mean Diurnal Relative Humidity Change Index

The mean diurnal relative humidity change index (I_{RH}) is defined as the mean amplitude of the diurnal relative humidity cycles at the exposed paint surface during a given time period. The amplitudes (difference between the maximum and minimum diurnal surface relative humidities) for the surface relative humidity cycles are calculated, and the arithmetic mean for these amplitudes is subsequently calculated. Diurnal relative humidity swings of the exposed paint surface are believed also to produce expansion/contraction cycles that can lead to fatigue-stress degradation of a paint layer.

Time of Wetness Index

The time of wetness index (I_{TOW}) is defined as the cumulative time during which the surface of a polymer coating is considered to be wet, i.e., the surface relative humidity is above 97%.* This index can be expressed mathematically by the following expression:

$$I_{TOW} = \sum_{i=1}^{n} \Delta_i t \qquad (20)$$

where $\Delta_i t$ is the length of time ($t_i - t_{i-1}$) during which the surface of a panel is wet.

SIMULATION RESULTS

Illustrative Six-Day Winter Period

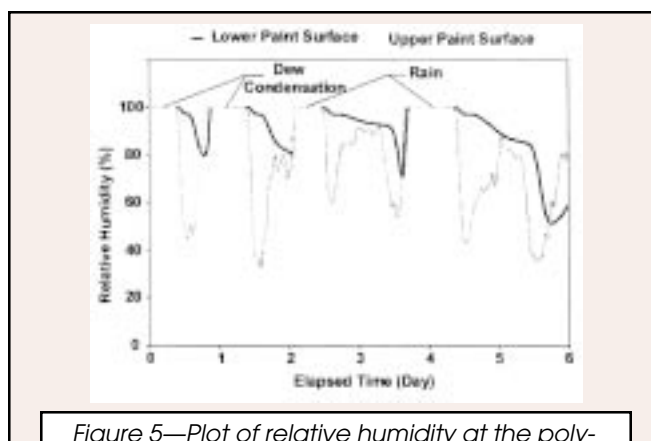The MOIST 4.0 model was first used to investigate the performance of the alkyd resin paint exposed to a six-day

winter period (January 9-14) in Miami, FL. A plot of the outdoor temperature and net incident solar radiation versus elapsed time is given in *Figure* 2. In *Figure* 3, the temperature calculated for the exposed surface of the alkyd resin paint is plotted versus elapsed time. The diurnal fluctuations in surface temperature were predominantly caused by the solar load on the surface, because the outdoor temperature was surprisingly steady during this period (see *Figure* 2). These diurnal variations in surface temperature will cause the alkyd resin paint to expand and contract, thereby potentially leading to fatigue-stress degradation. The outdoor dew point temperature is also plotted in *Figure* 3. The surface temperature fell below the

a. Average outdoor temperature and hourly solar radiation

b. Wetting hours by dew condensation and rain
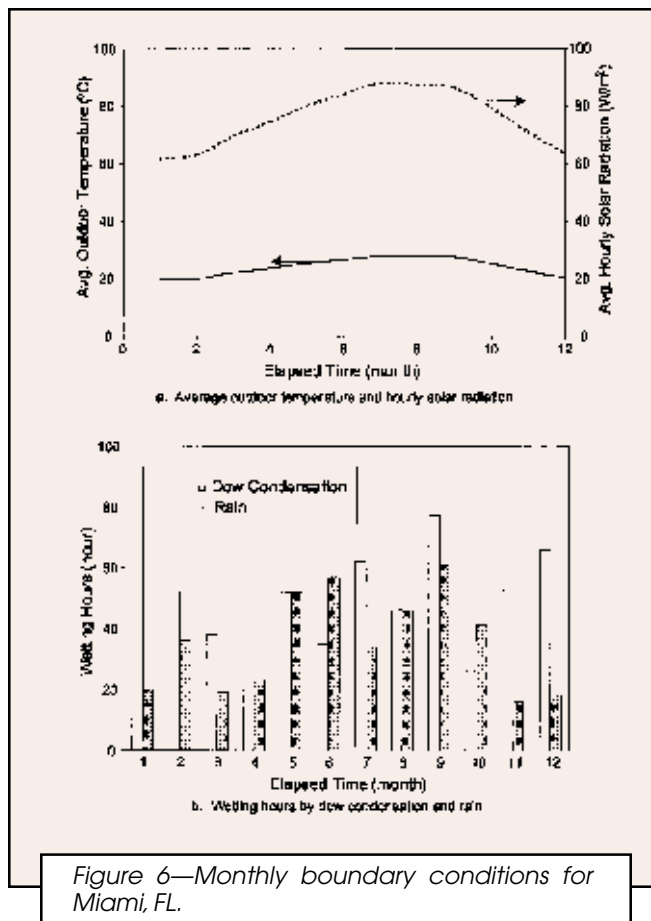
Figure 6—Monthly boundary conditions for Miami, FL.

*When the relative humidity is above 97%, the Kelvin equation indicates that liquid water appears in the large pore space of a material.

outdoor dew point temperature during several periods due to thermal radiation exchange between the surface and a cold night sky. Under this condition, dew condensation wets the exposed paint surface. Periods during which dew condensation occurred are depicted by the horizontal line segments shown in *Figure* 3. Several periods of rain occurred during the second and third day that also wetted the exposed paint surface, as indicated at the bottom of the graph.

The predicted moisture contents at the upper and lower paint surfaces are plotted versus elapsed time in *Figure* 4. Dew condensation and rain caused the moisture content at both the upper and lower surfaces to saturate. However, the surfaces dried out quickly during sunny periods of the following day. The lower surface dried more slowly than the upper surface because of the vapor transfer resistance of the paint. These abrupt wetting and drying cycles will cause the alkyd resin paint to swell and shrink, thereby leading to potential fatigue-stress degradation. Furthermore, when paint becomes wet, chemical degradation related to the presence of water (e.g., hydrolysis) can oc-

cur, while other chemical degradation mechanisms can be accelerated.[1]

The predicted relative humidity at the upper and lower paint surfaces are plotted versus elapsed time in *Figure* 5. Variations in relative humidity occurred at both the upper and lower paint surfaces, although the variations at the lower surface were considerably smaller in comparison. This factor might contribute to the higher amounts of degradation that often occur at the upper paint surface compared to the lower paint surface. The lower paint surface is unable to completely dry out during warm day periods and remains in a partially wet state, with the relative humidity often above 80%. Laboratory experiments conducted at the National Institute of Standards and Technology have indicated that ultraviolet (UV) photolytic degradation rates are significantly increased at elevated relative humidity. The elevated lower surface relative humidity might enhance photolytic degradation, provided that UV radiation is able to penetrate the paint and reach the lower paint surface.[1]

Annual Variation of the Damage Indices

HOT AND HUMID CLIMATE (MIAMI, FL): The new model was used to investigate the annual variation of the damage indices for a hot and humid climate (Miami, FL). The monthly boundary conditions are shown in *Figure* 6. The daily-average outdoor temperature and solar radiation are given in *Figure* 6a, while the hours of wetting by dew condensation and rain are given in *Figure* 6b. A total of 640 hr of dew condensation and 423 hr of rain occurred in
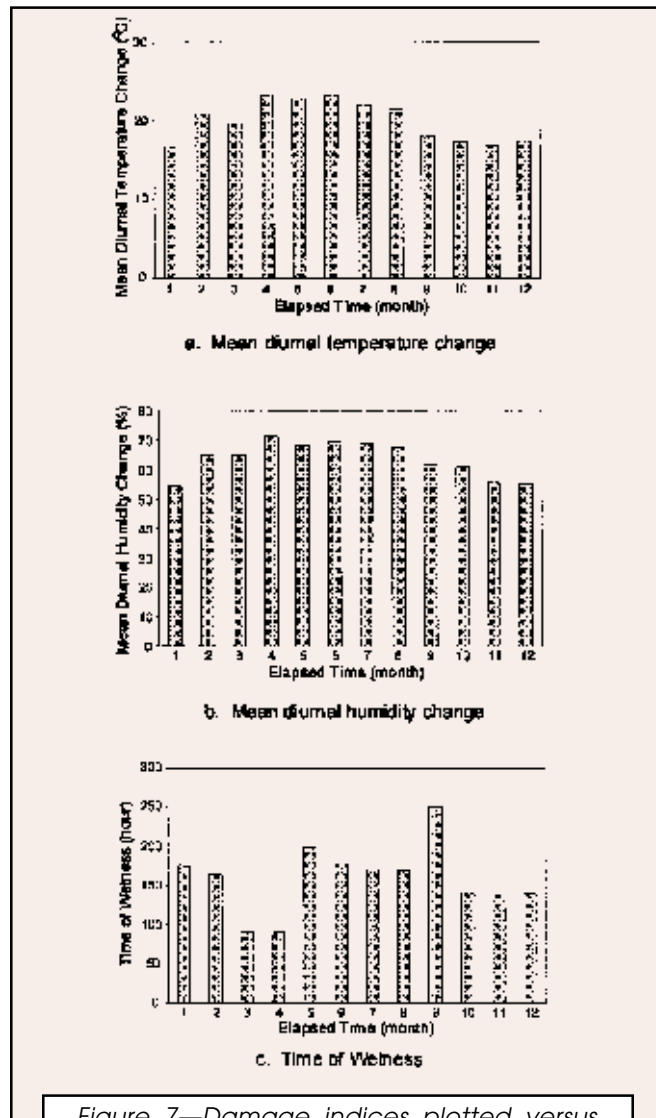

Figure 7—Damage indices plotted versus months of the year for Miami, FL. The first month is January.
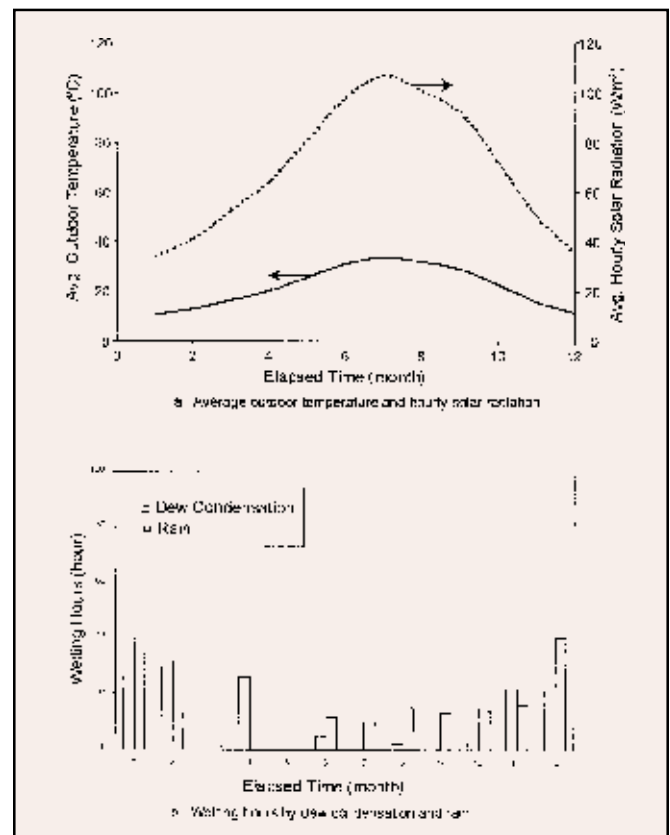

Figure 8—Monthly boundary conditions for Phoenix, AZ.

Miami, FL during this one-year period. Thus, surface wetness was caused more by dew condensation than by rain.

The three damage indices are plotted versus time for the one-year period in *Figure* 7. In these plots, the first month is January. The mean diurnal temperature change index (*Figure* 7a) and mean diurnal humidity change index (*Figure* 7b) attained a maximum during the summer (center of the plot) caused by the larger amount of solar heating of the exposed paint surface during the summer. These two indices did not vary significantly with the time of year in Miami, FL due to the relatively small variations in solar radiation. However, the time of wetness index (*Figure* 7c) varied considerably with time of year, attaining a low value of 91 hr in April and reaching a maximum value of 251 hr in September. These variations were a direct consequence of surface wetting by dew condensation and rain.

HOT AND DRY CLIMATE (PHOENIX, AZ): The new model was also used to investigate the annual variation of the damage indices for a hot and dry climate (Phoenix, AZ). The monthly boundary conditions are shown in *Figure* 8.
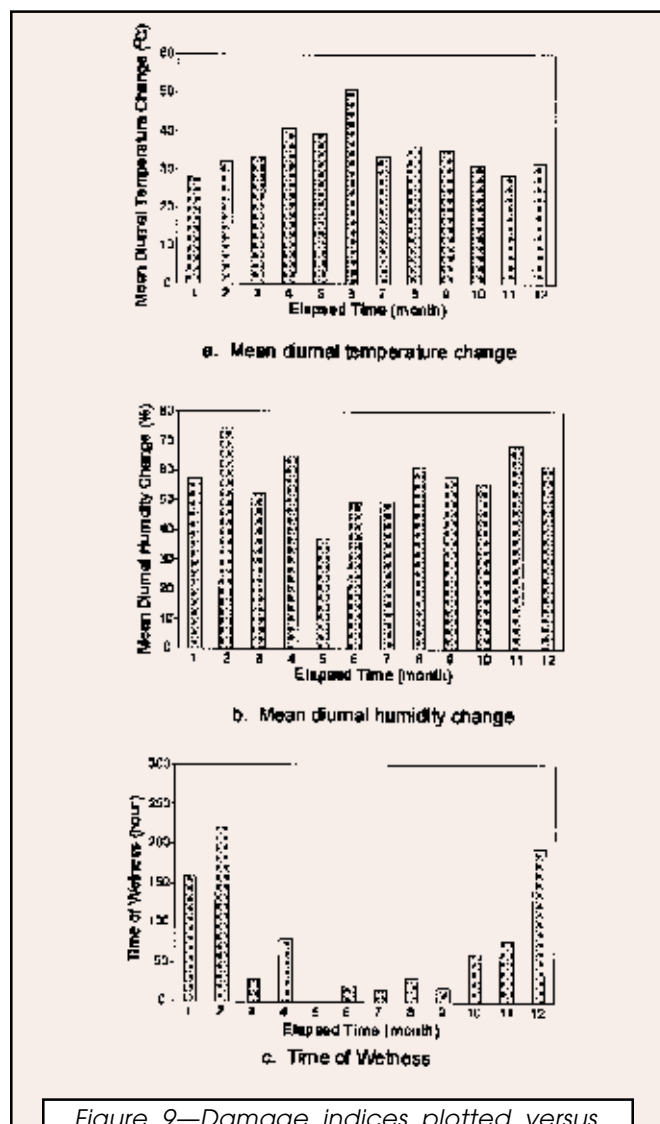
Comparing *Figures* 6a and 8a, the average outdoor temperature is lower during the winter in Phoenix than in Miami. Additionally, the solar radiation during the summer is considerably higher in Phoenix than in Miami because of the predominantly clear sky conditions. Comparing *Figures* 6b and 8b, considerably less surface wetting occurs by dew condensation and rain in Phoenix than in Miami, and the surface wetness during the summer period is particularly low in Phoenix. The yearly total number of hours of dew condensation and rain were 159 and 216, respectively, for the one-year period in Phoenix.

The annual variations of the damage indices for Phoenix, AZ are plotted in *Figure* 9. The mean diurnal temperature change index in Phoenix, AZ (see *Figure* 9a) was always much higher than that in Miami, FL. This difference was caused by a larger diurnal ambient temperature swing in Phoenix due to higher solar radiation per month during the summer compared to Miami. A higher mean diurnal temperature change index means that the paint will experience more fatigue-stress degradation due to contraction and expansion cycles induced by the surface temperature cycling. The mean diurnal humidity change

a. Mean diurnal temperature change

b. Mean diurnal humidity change

c. Time of Wetness

Figure 9—Damage indices plotted versus months of the year for Phoenix, AZ. The first month is January.

a. Solar radiation

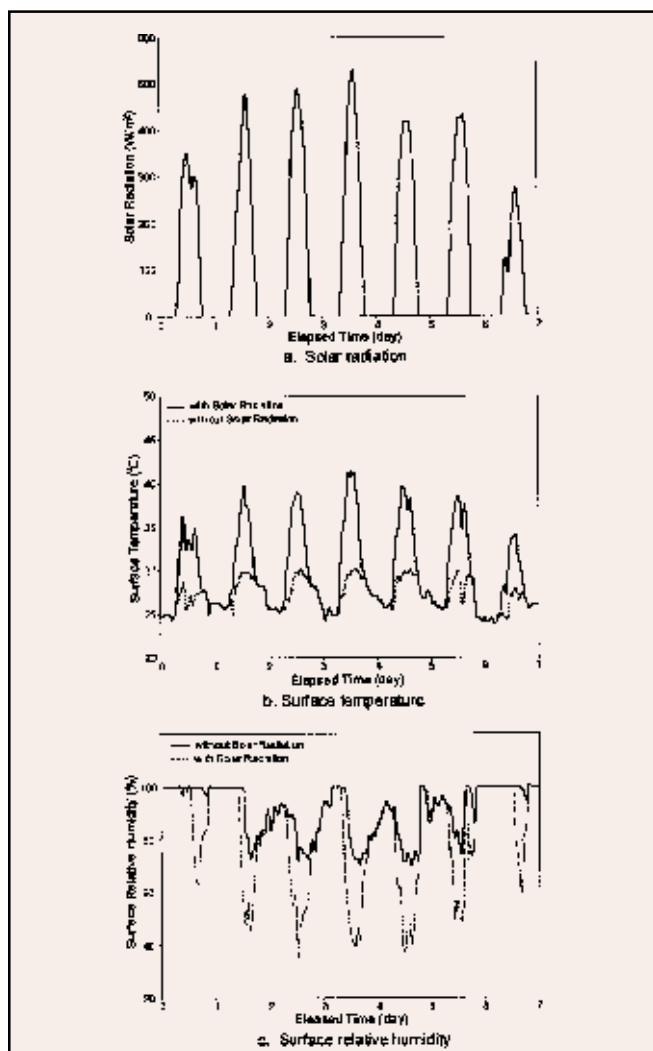b. Surface temperature

c. Surface relative humidity

Figure 10—Illustration of the effect of solar radiation on surface temperature and surface relative humidity during first week of September in Miami, FL.

index in Phoenix, AZ (see *Figure* 9b) has about the same magnitude as that in Miami FL. Thus, the fatigue-stress degradation due to contraction and expansion cycles induced by humidity cycling will be very similar for the two climates. The time of wetness index in Phoenix, AZ (see *Figure* 9c) is considerably lower than that of Miami, FL, particularly during the summer.

In summary, exposure in Phoenix, AZ is associated with a much larger mean diurnal temperature change index compared to exposure in Miami, FL, and diurnal expansion/contraction cycles are more of a factor contributing to degradation. On the other hand, paint exposed in Miami, FL experiences much more surface wetting, particularly under high temperature conditions. As a result, chemical reactions (e.g., hydrolysis) are more likely to be a factor contributing to degradation in Miami, FL.

Factors Affecting Damages Indices

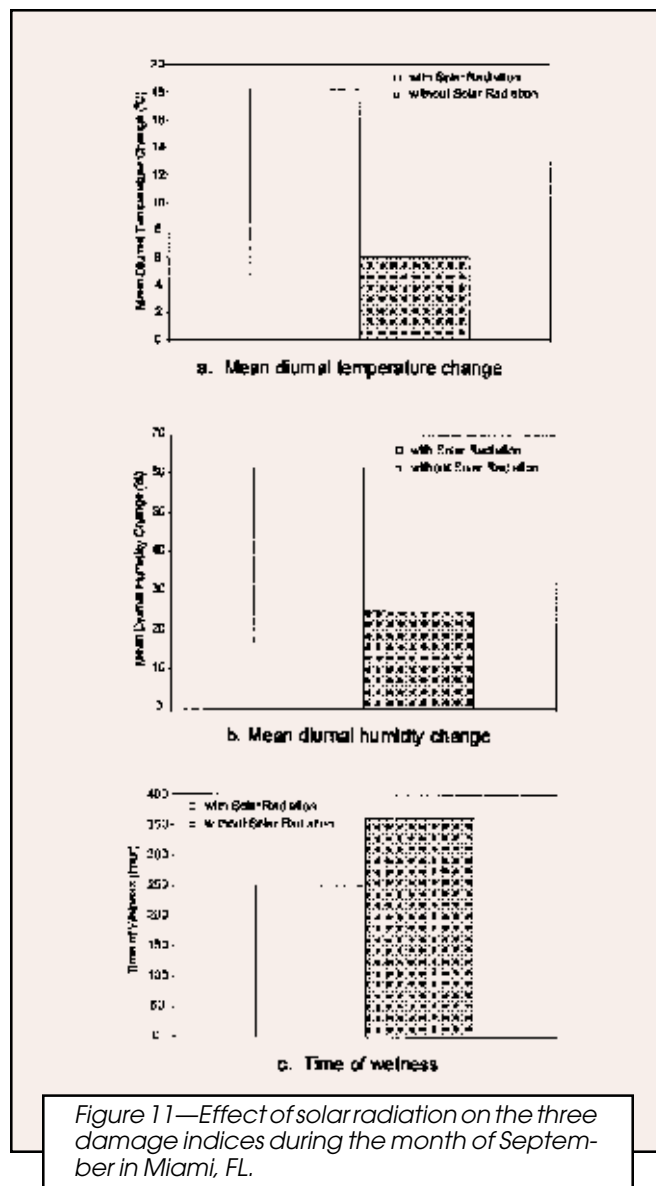The computer model was then used to investigate the effect of solar radiation, surface wetting by rain and dew

Figure 11—Effect of solar radiation on the three damage indices during the month of September in Miami, FL.

condensation, and variations in outdoor temperature and relative humidity on the three damage indices. The period selected for analysis was month 9 (September) of Miami, FL because this period had a very high time of wetness index and mean diurnal humidity change index, thereby indicating a high potential for degradation.

SOLAR RADIATION: The effect of incident solar radiation on the temperature and relative humidity at the exposed paint surface was examined for the first week of September. The variation in solar radiation is plotted in *Figure* 10a. The diurnal variation in surface temperature is plotted in *Figure* 10b for cases with and without solar radiation. The presence of solar radiation greatly increased the amplitude of diurnal fluctuations in surface temperature. When solar radiation was removed from the computer simulation, the variation in surface temperature became

NOMENCLATURE

a	empirical exponent	dimensionless
A_i	empirical constants (i=1 to 3)	—
c	specific heat	J/kg·°C
E	emittance factor $[1/(1/e_s+1/e_{sky}-1)]$	dimensionless
D	liquid diffusivity	m²/s
D'	modified liquid diffusivity, $D' = D (\gamma_s - \gamma_{97})$	m²/s
h_c	convective heat transfer coefficient	W/m²·°C
h_{lv}	latent heat of vaporization	J/kg
h_m	vapor mass transfer coefficient	kg/s·m²·Pa
h_r	radiation coefficient	W/m²·°C
H	height above the ground	m (ft)
H_{sol}	incident solar hemispherical radiation	W/m²
I_{RH}	mean diurnal humidity change index	% relative humidity
I_T	mean diurnal temperature change index	°C
I_{TOW}	time of wetness index	h
k	thermal conductivity	W/m·°C
M	vapor permeability	kg/s·m²·Pa
p	vapor pressure	Pa
q	heat flux rate	W/m²
rh	relative humidity	dimensionless
s	relative saturation $[s = (\gamma-\gamma_{97})/(\gamma_s-\gamma_{97})]$	dimensionless
t	time	s
T	temperature	°C
TCC	total cloud cover	dimensionless
U	wind speed	m/s
y	distance	m
α	solar absorptance	dimensionless
γ	moisture content	kg_w/kg_d
η_l	liquid flux rate	kg/s·m²
η_v	vapor flux rate or water vapor transfer rate	kg/s·m²
μ	vapor permeability	kg/s·m·Pa
ρ	density	kg/m³
σ	Stefan-Boltzmann constant	W/m²·K⁴

Subscripts

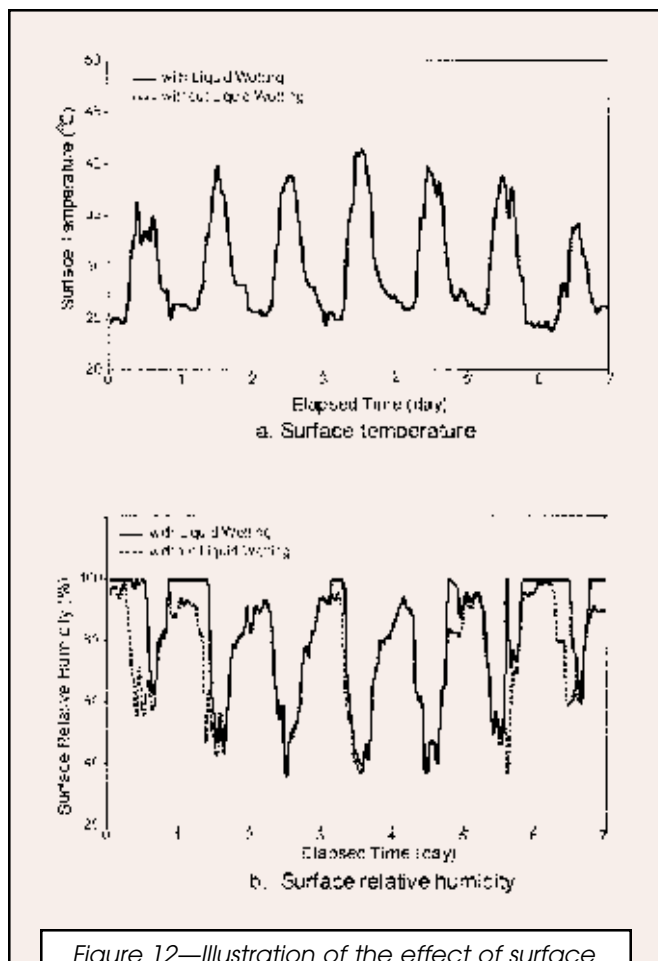|	
d	dry material
clear	clear condition
e	effective value
i	indoor
o	outdoor
p	paint property
ref	reference value
s	surface or saturated
sky	sky
w	wet or water
97	maximum sorption (rh = 97%)

Figure 12—Illustration of the effect of surface wetting (rain and dew condensation) on surface temperature and surface relative humidity during the first week of September in Miami, FL. Note that in (a), the two curves overlap.

quite small. The variation in relative humidity at the exposed paint surface is shown in *Figure* 10c. In a similar way, the presence of solar radiation significantly increased the amplitude of the diurnal fluctuation in surface relative humidity. When solar radiation impinges onto the exposed paint surface, it elevates the surface temperature, thereby causing the surface to undergo considerably more drying than the same surface without solar radiation. Furthermore, the presence of solar radiation dries a paint film and, thus, reduces its time of wetness (i.e., surface relative humidity greater than 97%).

The effect of solar radiation on the three damage indices during the month of September in Miami, FL, is shown in *Figure* 11. The light colored bars depict the magnitude of the indices with solar radiation, while the dark colored bars denote the magnitude of the indices without solar radiation. The presence of solar radiation increased the mean diurnal temperature change index from 6.0°C to 18.3°C. Similarly, the presence of solar radiation increased the mean diurnal humidity change index from 24.7% relative humidity to 61.5% relative humidity. These increases in temperature and humidity cycling are believed to produce much larger expansion/contraction cycles, thereby potentially causing considerably higher fatigue-stress degradation. On the other hand, the presence of solar radia-

tion is seen to decrease the time of wetness index from 363 hr to 251 hr. Without knowing the relative contribution of the three damage indices on paint degradation, determining the overall effect of solar radiation on degradation is not possible.

SURFACE WETTING: The effects of surface wetting (by rain and dew condensation) on the surface temperature and surface relative humidity of the exposed paint surface were examined for the first week of September. As shown in *Figure* 12a, surface wetting of the exposed paint surface by rain or dew condensation had little or no effect on surface temperature.* The two diurnal curves are virtually the same. In *Figure* 12b, surface wetting had a small effect on the magnitude of the diurnal relative humidity fluctuations. When surface wetting is not present, the surface still reaches a very high relative humidity due to water vapor adsorption. The temperature difference between the surface and ambient air (due to radiation exchange between the surface and a cold night sky) causes water vapor transfer from the ambient air to the surface. However, during periods of surface wetting by rain and dew condensation, additional moisture is transferred to the surface, and the surface relative humidity becomes saturated. As a result, the time of wetness of the paint surface is significantly increased.

The effect of surface wetting by rain and dew condensation on the three damage indices during the month of September is shown in *Figure* 13. As shown in *Figure* 13a, the mean diurnal temperature change index is unchanged. In *Figure* 13b, the presence of surface wetting only slightly increases the mean diurnal humidity change index, which is consistent with the small reductions in the diurnal relative humidity cycles (shown in *Figure* 12b above). On the other hand, the presence of liquid wetting at the exposed paint surface substantially increases the time of wetness index, as shown in *Figure* 13c. When surface wetting is not present, the time of wetness index is still greater than zero, because the surface relative humidity can rise above 97% due to water vapor adsorption from the ambient air to the surface (induced by the temperature difference between the surface and the ambient air).

These results reveal that the presence of surface wetting by rain and dew condensation produces a considerable rise in the time of wetness index, thereby increasing the potential for chemical degradation. However, surface wetting had a small and unimportant effect on the mean diurnal temperature change index and the mean diurnal humidity change index.

Effect of Variation in the Outdoor Ambient Temperature and Relative Humidity

Finally, the computer model was used to study the effects of variations in outdoor temperature and relative humidity on the three damage indices. The effects of solar radiation, surface wetting by rain and dew condensation, and surface wetting by vapor adsorption were removed from the simulations. The remaining outdoor weather parameters affecting the results were variations in out-

---

*In the model, the cooling of the exposed surface by the impingement of rain below ambient temperature was neglected. Water evaporates from falling raindrops causing them to have a temperature below the ambient air.
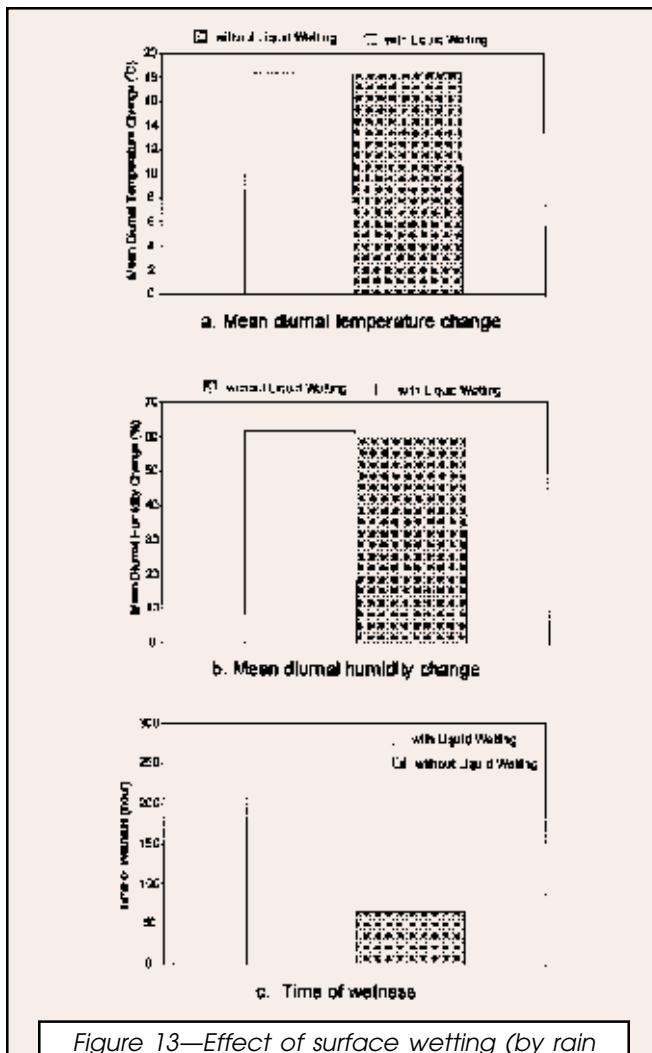
Figure 13—Effect of surface wetting (by rain and dew condensation) on the three damage indices during the month of September in Miami, FL.
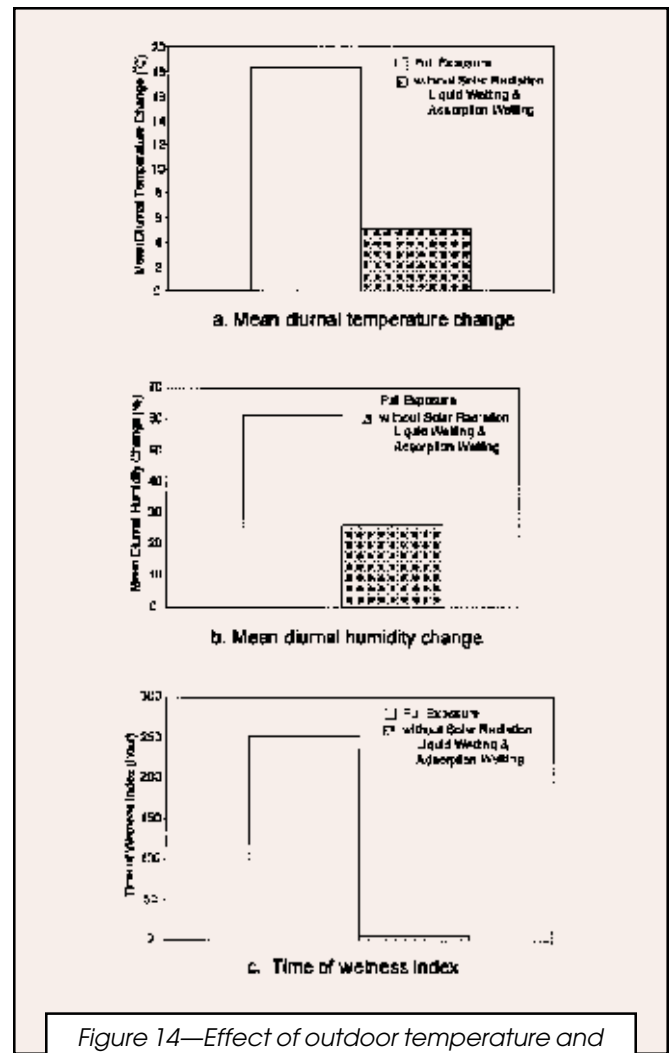

Figure 14—Effect of outdoor temperature and relative humidity on the three damage indices for the month of September (excluding solar radiation and surface wetting by rain and dew condensation) in Miami, FL.

door temperature and relative humidity. This simulation reflects the situation in which the exposed paint surface is shielded by a horizontal surface.

The effect of variations in the outdoor temperature and relative humidity on the three damage indices is shown in *Figure* 14 for the month of September in Miami, FL. The dark colored bars depict performance without solar radiation and surface wetting, while the light colored bars denote performance with full exposure to all parameters of the outdoor weather. As shown in *Figure* 14, the mean diurnal temperature change index was reduced from 18.3 to 5.1°C. This reduction was primarily caused by the elimination of solar heating of the surface during warm day periods. The mean diurnal humidity change index was also reduced from 61.5 to 26.4%, and the time of wetness index was reduced from 251 hr to 6 hr. The very small amount of wetting of the surface is due to vapor adsorption by the surface from the humid ambient air (surface relative humidity greater than 97%) at the same temperature.

These results reveal that when the effects of incident solar radiation and surface wetting by rain and dew con-

densation are removed from the computer simulations, variations in outdoor temperature and relative humidity possess a much smaller mean diurnal temperature change index and mean diurnal humidity change index.

SUMMARY AND CONCLUSIONS

A new heat and moisture transfer model, called MOIST 4.0, was presented that predicts the temperature, moisture content, and relative humidity of a polymer coating applied to a substrate as a function of position and time. Vapor transport was modeled using water vapor pressure as a potential with vapor permeability serving as a transport coefficient. Capillary (liquid) flow was modeled using relative saturation as a potential with the "modified" liquid diffusivity serving as a transport coefficient. The model also included the wetting at the exterior surface by rain and dew condensation and the important effect of incident solar radiation. Convection at the exposed paint surface was calculated from the local wind speed. Hourly outdoor weather parameters were obtained from either

WYEC files, TMY files, or measured parameters at an outdoor exposure site.

This new model was used to study several of the adverse effects of climate on the potential degradation of an alkyd-resin paint exposed to outdoor weather conditions. The following three damage indices were introduced to quantify adverse effects of climate: a mean diurnal temperature change index, a mean diurnal humidity change index, and a time of wetness index. The variation of these indices as a function of time of year was investigated for a hot and humid climate (Miami, FL) and a hot and dry climate (Phoenix, AZ). In addition, the relative effects of solar radiation, surface wetting by rain and dew condensation, and variation in the outdoor temperature and relative humidity were investigated.

The computer simulations revealed that exposure in Phoenix, AZ cause a much larger mean diurnal temperature change index compared to exposure in Miami, FL. On the other hand, paint exposed in Miami, FL experienced much more surface wetting, particularly under high temperature conditions. As a result, chemical reactions (e.g., hydrolysis) are more likely to be a factor contributing to degradation of the alkyd resin paint in Miami, FL.

The presence of solar radiation and surface wetting by rain and dew condensation was found to contribute significantly to the adverse effects of the outdoor climate. When these weather parameters were removed from the computer simulations, the three damage indices were substantially reduced. However, the variation of the outdoor temperature and relative humidity had some residual contribution to the damage indices.

NIST is planning to conduct a series of experimental measurements to verify the accuracy of the new model.

ACKNOWLEDGMENTS

References

(1) Martin, J.W., Nguyen, T., Byrd, W.E., and Embree, E., "Relating Laboratory and Outdoor Exposure of Coatings II: Effect of Relative Humidity on Photodegradation of Acrylic-Melamine Coatings," *Polym. Degrad. Stab.*, submitted in 2000.
(2) Burch, D.M. and Martin, J.W., "Predicting the Temperature and Relative Humidity of Polymer Coatings in the Field," *Service Life Prediction of Organic Coatings—A Systems Approach*, American Chemical Society Symposium Series 722, Breckenridge, CO, 85 (1997).
(3) Burch, D.M. and Chi, J., "MOIST: A PC Program for Predicting Heat and Moisture Transfer in Building Envelopes (Release 3.0)," *NIST Special Publication 917*. National Institute of Standards and Technology, Gaithersburg, MD (1997).
(4) International Energy Agency, Annex 24, "Heat, Air and Moisture Transfer in Insulated Envelope Parts," Final Report (Task 1 – Modeling) (1996).
(5) Duffie, J.A. and Beckman, W.A., *Solar Engineering of Thermal Processes*, Second Ed. John Wiley & Sons, Inc., New York, 1991.
(6) Pedersen, C.R., "Combined Heat and Moisture Transfer in Building Constructions," Report No. 214, Technical University of Denmark (1990).
(7) Richards, R.F., "Measurement of Moisture Diffusivity for Porous Building Materials," *Proc. ASHRAE/DOE/BTECC Conference on the Thermal Performance of the Exterior Envelopes of Buildings V*, Clearwater Beach, FL (1992).
(8) ASHRAE, *1997 ASHRAE Handbook—Fundamental*, American Society of Heating, Refrigerating and Air Conditioning Engineers, Inc., Atlanta (1997).
(9) Crow, L.W., "Development of Hourly Data for Weather Year for Energy Calculations (WYEC)," *ASHRAE Journal*, 23, No. 10, 34 (1981).
(10) Marion, W. and Urban, K., "User's Manual for Typical Meteorological Years," National Renewable Energy Laboratory (1995).
(11) Bliss, R.W., "Atmospheric Radiation Near the Surface of the Ground," *Solar Energy*, 5, 103 (1961).
(12) Galbraith, G.H. and McLean, R.C., "Interstitial Condensation and the Vapor Permeability of Building Materials," *Energy and Buildings*, 14, 193 (1990).
(13) Gubareff, G.G., Janssen, J.E., and Torborg, R.H., "Thermal Radiation Property Survey," Second Ed., Honeywell Research Center, Minneapolis, MN, 1960.
(14) Rosen, H.N. and Martin, J.W., "Sorption of Moisture on Epoxy and Alkyd Free Films and Coated Steel Panels," JOURNAL OF COATINGS TECHNOLOGY, *63*, No. 792, 85 (1991).
(15) Valen, M.S., "Moisture Transfer in Organic Coatings on Porous Materials: The Influence of Varying Environmental Conditions," Thesis for Doctoral Degree in Engineering, The Norwegian University of Science and Technology (1998).